Structural Eng. / Earthquake Eng. Vol. 5. No. 1, 11s-20s. April 1988
Japan Society of Civil Engineers (Proc. of JSCE No. 392/I-9)

AN EXPERIMENTAL STUDY ON STRENGTH OF STEEL SHEET PILE MODELS UNDER REPETITIVE COMPRESSION

By Eiichi WATANABE, Masakazu FUKUWAKA**, Hidenori ISAMI*** and Yoshio FUKUMORI*****

This paper presents an experimental investigation on the buckling strength of stub channel columns under repetitive compression to determine reasonable cross sections of steel sheet piles against the repeated driving force by diesel hammer. The tests were performed under the pseudo-static condition using microcomputer-based servo-controlled testing system to find the deteriorating properties of steel sheet pile models undergoing the large elasto-plastic deformations under repetitive compression.

Through the study, the deteriorating properties of the sheet pile model were clarified and found to be influenced by the width-thickness ratio, aspect ratio of the flange plates, and the relative dimensioning of the web and flanges.

Keywords : *local buckling, sheet piles, repetitive compression*

1. INTRODUCTION

Nowadays, steel sheet piles are being used increasingly at various construction sites such as for buildings, bridges, highways and wharfs. The recent trend of the sheet piles, especially in the European countries and USA, is the increased use of products of wider web. Thus, the chances are the efficiency of pile driving being hindered by the local buckling near the cap : Once the piles buckle they can not be driven any more into the soil foundation[1].

Steel sheet piles are used as structural members essentially to resist the bending moments caused by the earth and water hydraulic pressures ; but not too much design considerations have been given against bucklings although they may be subjected to large repeated hammer drive forces and seriously damaged.

The current interest of study herein is to determine reasonable and optimal cross sections of the sheet piles invulnerable and strong enough against the repeated severe drivings by diesel hammer. Although rigorously speaking, the effects of the impact and the inertia forces have to be taken into account, and there seem to be several differences in stress-strain relationships between the dynamic and static responses of steel structures[2)~4)], this study is only concerned with the cyclic assault of axial compression to give the first approximation to the problem. The experiments reported herein have been conducted using an automated structural testing system and the specimens are designed as stub channel columns under repetitive compressive force[5),6)], however, being applied in the static condition.

* Member of JSCE, Ph. D. & Dr. Eng., Professor, Kyoto University (Yoshida-Honmachi, Sakyo, Kyoto 606)
** Member of JSCE, M. S., Engineer, Kawasaki Steelwork, Inc. (2-2-3, Uchisaiwai, Chiyoda, Tokyo 100)
*** Member of JSCE, Dr. Eng., Associate Professor, Kohchi National College of Technology (200-1, Monobe-Otsu, Nangoku, Kohchi 783)
**** Member of JSCE, M. S., Osaka Prefecture Government (2, Ohtemae, Higashi, Osaka 540)

2. DESCRIPTIONS OF TESTS

(1) Design of test specimens

The test stub columns of channel cross section are so designed as to be classified into six types by two different flange heights and three different flange thicknesses. For each type of the specimens, identical specimens are fabricated using ordinary carbon steel of SS 41 with one being for the test of residual stress and the rest being for the loading tests.

The following points are considered in the design :

(1) to maintain the cross-sectional profile of the prototype sheet piles such as the aspect and width-thickness ratios as much as possible,

(2) to make the local buckling occur in the elasto-plastic domain,

(3) to keep the magnitude of the initial out-of-plane deflection as low as the prototype ; hence, too thin plates should not be used,

(4) to neglect the effect of the outstanding edge stiffeners ; thus, the specimens are designed to be of open channel cross section, and

(5) to restrict the size of the specimens so that the testing can be performed within the static capacity of the testing machine, namely, 40 tf (392.24 kN) in both vertical and horizontal directions.

The local buckling strength of the flange plate of channel cross-sectional columns was calculated first to determine the cross section of the test specimens. According to Bleich, it can be given by the following : [7]

$$\sigma_{cr}=\sqrt{\tau}\,\frac{\pi^2 KE}{12(1-\nu^2)}\left(\frac{t_f}{h}\right)^2 \qquad (1)$$

where

$K=p+2\sqrt{q}$: buckling coefficient, and

$$\zeta=\frac{b}{h}\left(\frac{t_f}{t_w}\right)^3\frac{1}{1-0.106[bt_f/(ht_w)]^2}$$

in which b, h, t_f and t_w refer to the width of the web, height of the flange, thickness of the flange and the thickness of the web, respectively. Moreover, τ designates the tangent modulus factor and becomes unity for elastic state. The values of p and q have been obtained and provided in a chart for different values of ζ by Bleich[7].

Table 1 tabulates the dimensions of the test specimens, CH 235 to CH 475, and those of several prototype sheet piles, KSP-5 L, KSP-6 L and KSP-7 L. As for the naming of the test specimen, CH 235, for example, implies that it is of channel cross section and t_f=2.3 mm and h=50 mm. The length of the stub column specimens was taken to be 600 mm. Moreover, assuming the flange plates to be one unloaded edge free and the other three edges simply supported, and thus taking the elastic buckling coefficient K=0.43, the non-dimensionalized parameters b/h, t_w/t_f and the generalized width-thickness ratio, R, can be evaluated as shown in Table 2. It may be seen that the R-values of the prototype sheet piles, being nearly unity, are well within the range of those of the test specimens from 0.65 to 1.78 so that the optimal value of R could be found within this range of R-values.

The end plates are welded to the ends of each stub column specimen, precisely ground and carefully polished. The lower end of the specimen is designed to be simply supported on a spherical bearing using the special clamp as illustrated in Fig. 1 (a). To remove the eccentricity, the bearing is made adjustable by three screws as illustrated in Fig. 1 (b). Furthermore, the upper end of the specimen is so designed that it receives the compressive force from the actuator ; it is free from the twisting moment, but can be considered to be clamped against bending.

(2) Standard material tests and residual stress tests

From the standard JIS coupon tests, it is found that the material behaves perfectly elasto-plastically with the yielding stress of 2 862 kgf/cm^2, 2 725 kgf/cm^2, 2 918 kgf/cm^2 and 2 734 kgf/cm^2 for the thickness

of 2.3 mm, 3.2 mm, 4.5 mm and 6.0 mm, respectively.

The residual stress tests were conducted to find the distribution of the residual stress using electric strain gauges by stress relieving method through cutting out strips from the central part of each specimen. Fig. 2 shows an example of the distribution of the longitudinal residual stresses in the cross section of CH 325, comparing with the residual stresses predicted by the formula with $\sigma_r = 0.41\,\sigma_Y$.

(3) Procedure of loading tests

The servo-controlled testing system automated by microcomputers is utilized herein. The testing system

Table 1 Dimensions of Test Specimens.

Specimen	t_f(mm)	h(mm)	t_w(mm)	b(mm)
CH235	2.3	50.0	6.0	100.0
CH325	3.2	50.0	6.0	100.0
CH455	4.5	50.0	6.0	100.0
CH237	2.3	70.0	6.0	100.0
CH327	3.2	70.0	6.0	100.0
CH457	4.5	70.0	6.0	100.0
KSP-5L	12.9	222.0	24.2	305.2
KSP-6L	13.6	249.0	27.6	285.6
KSP-7L	14.8	274.0	29.5	273.8

t_f : *Thickness of flange*
h : *Hight of flange*
t_w : *Thickness of web*
b : *Width of web*

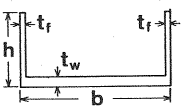

Table 2 Non-dimensionalized Parameters of Test Specimens.

Specimen	b/h	t_w/t_f	R
CH235	2.00	2.61	1.26
CH325	2.00	1.88	0.90
CH455	2.00	1.33	0.65
CH237	1.43	2.61	1.78
CH327	1.43	1.88	1.28
CH457	1.43	1.33	0.91
KSP-5L	1.37	2.21	1.00
KSP-6L	1.15	2.03	1.06
KSP-7L	1.00	2.27	1.07

R : *Generalized slenderness ratio of flange plate*

$$R = \frac{h}{t_f}\sqrt{\frac{12(1-\nu^2)\sigma_Y}{\pi^2 k E}}$$

k : *Buckling coefficient*
ν : *Poisson's ratio*

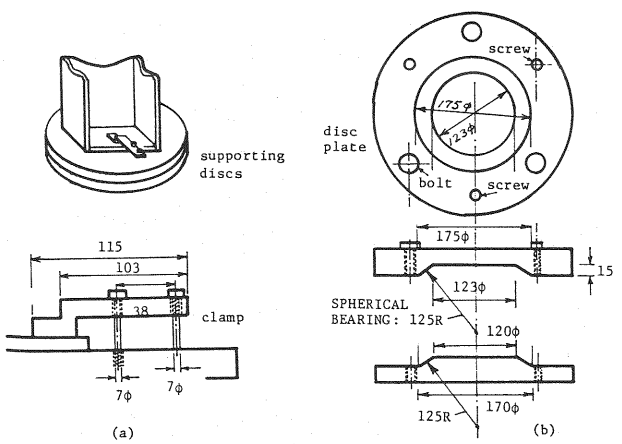

Fig. 1 End Support.

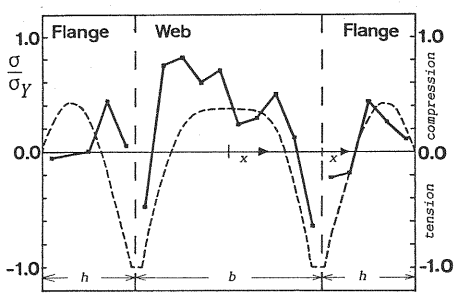

Experimental form
Idealized form as follows:

Idealized Residual Stress Distributions

Web

$$\sigma = \begin{cases} \sigma_Y \left[\cos \frac{\pi}{m} \left(\frac{x}{b} \right)^2 - 1 \right] + \sigma_r & \text{when } \sigma > -\sigma_Y \\ -\sigma_Y & \text{when } \sigma \leq -\sigma_Y \end{cases}$$

where $-1/2 \leq x/b \leq 1/2$ *and* m *can be determined from the longitudinal self-equilibrium.*

Flange

$$\sigma = \begin{cases} \sigma_Y \left[\cos a_3 \left(\frac{x}{h} - a_1 \right) - 1 \right] + \sigma_r & \text{when } \sigma > -\sigma_Y \\ -\sigma_Y & \text{when } \sigma \leq -\sigma_Y \end{cases}$$

where $0 \leq x/h \leq 1$, $a_3 = a_1 + a_2$, $\cos \pi a_1 = \sigma_r$ *and* $\cos \pi a_2 = 1 - \sigma_r$.

Fig. 2 Residual Stress Distributions. Measurement for CH 325 and Idealized Form $\sigma_r = 0.41\,\sigma_Y$.

consists of three groups of servo testing machine group, data acquisition group and micro computer group, and the details of the software and hardware of the system have been reported by Watanabe et al. [5),6)].

3. RESULTS OF LOADING TESTS

(1) Failure types and out-of-plane deflections

Table 3 summarizes the main test results such as the number of cycles, the maximum load, the specified boundary condition at the upper end, the type of collapse and the location L_c and the width h_c of the failure mechanism in Fig. 3. The width h_c is almost twice as the height h of the flange plate. The failure types of the specimens are shown to be mainly caused by the local and/or torsional bucklings of the flanges.

Fig. 4 shows an example of the out-of-plane deflections presented both in contour lines and in

Table 3 Failure Types and Failure Mechanisms.

Specimen	Cycle	Maximum Load (tonf)	Upper End Fixed	Type of Collapse	Location L_c (mm)* R	Location L_c (mm)* L	Width h_c (mm)** R	Width h_c (mm)** L
CH235A	3	22.96	-	Local	580(0.97)	588(0.98)	70(0.12/1.40)	65(0.11/1.30)
B	9	20.43	Fixed	Torsional	576(0.96)	27(0.05)	68(0.11/1.36)	62(0.10/1.24)
C	1	19.98	-	Torsional	582(0.97)	62(0.10)	75(0.13/1.50)	84(0.14/1.68)
CH325A	6	25.34	-	Local	321(0.54)	255(0.43)	105(0.18/2.10)	114(0.19/2.28)
B	6	23.36	Fixed	Local	332(0.55)	298(0.50)	108(0.18/2.16)	97(0.16/1.94)
C	1	22.24	-	Local	288(0.48)	321(0.54)	105(0.18/2.10)	103(0.17/2.06)
CH455A	6	28.11	Fixed	Torsional	557(0.93)	62(0.10)	103(0.17/2.06)	98(0.16/1.96)
B	9	29.41	-	Local	453(0.76)	354(0.59)	108(0.18/2.16)	92(0.15/1.84)
C	4	32.04	-	Local	540(0.90)	528(0.88)	121(0.20/2.42)	120(0.20/2.40)
CH237A	4	20.83	-	Local+Torsional	512(0.85)	196(0.33)	142(0.24/2.02)	120(0.20/1.71)
B	6	20.53	Fixed	Local+Torsional	313(0.52)	94(0.16)	156(0.26/2.23)	148(0.25/2.11)
C	1	20.45	-	Local+Torsional	332(0.55)	285(0.48)	- ***	- ***
CH327A	5	22.34	-	Local	354(0.59)	125(0.21)	145(0.24/2.07)	152(0.25/2.17)
B	10	23.33	Fixed	Local+Torsional	412(0.69)	188(0.31)	148(0.25/2.11)	142(0.24/2.03)
C	4	23.19	-	Local	335(0.56)	256(0.43)	143(0.24/2.04)	152(0.25/2.17)
CH457A	8	32.44	Fixed	Torsional	558(0.93)	68(0.11)	123(0.21/1.76)	132(0.22/1.89)
B	9	31.91	-	Local	492(0.82)	566(0.94)	154(0.26/2.20)	168(0.28/2.40)
C	4	32.94	-	Torsional	546(0.91)	65(0.11)	152(0.25/2.17)	163(0.27/2.33)

* The symbol 'R' and 'L' refer to the right and left flange plates of sheet piles, respectively. The value x in parenthesis (x) indicates the ratio of the length L_c to the overall length L=600mm.
** The value x in parenthesis (x/y) shows the ratio of the width h_c to L=600m, and the value y shows the ratio of h_c to the height of the flange plate h=50mm or 70mm.
*** These values can not be measured due to large deformations of the flange plates.

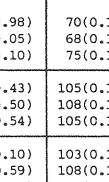

Fig. 3 Location L_c and Width h_c of Failure Mechanisms.

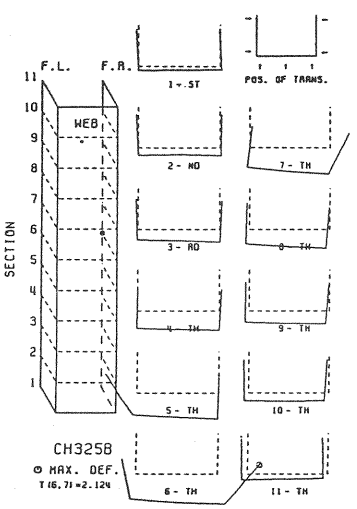

Fig. 4 Out-of-plane Deflections of CH325B in CYCLE=6.

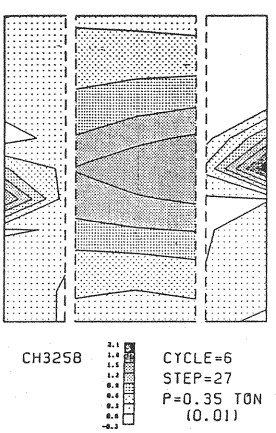

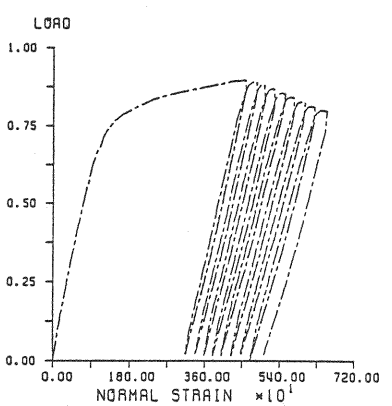

Fig. 5 Load-Axial Strain Curve of CH235B.

two-dimensional drawings, where the rigid-body motion has been eliminated. As a result of the formation of the failure mechanism associated with the local buckling and the subsequent loss of the global flexural rigidity about the weak axis, the web plate is seen to have undergone the global out-of-plane bending deflections.

(2) Load-displacement relationships and stress distributions

Fig. 5 shows an example of the relationship between the non-dimensionalized total load in terms of the yielding load and the axial strain of CH 235 B.

Figs. 6 show the distribution of axial stresses computed from the readings of strain gauges while assuming the residual stress distribution as shown in Fig. 2 and assuming the perfect elasto-plasticity of the steel for each step of loading. To make this possible, the web and each of the flanges are theoretically divided into 100 and 50 strips, respectively, for the interpolation to find the strain distributions. From the computed results, it is shown that the axial stress in the first cycle loading increases uniformly under compression. Then, the axial stress also decreases uniformly in the first cycle unloading. The residual deformations gradually tend to grow due to the plastic deformations accelerated under repetitive compression. As the number of cycles increases, the residual stress distribution seems to be leveled off in the cross section of the specimen, and the axial stress distributions near the free edge of each flange plate are shown to be virtually locked in due to the formation of the failure mechanisms in the flange plate.

Figs. 7 to 12 show the relationship between the non-dimensionalized applied load by the yielding load and

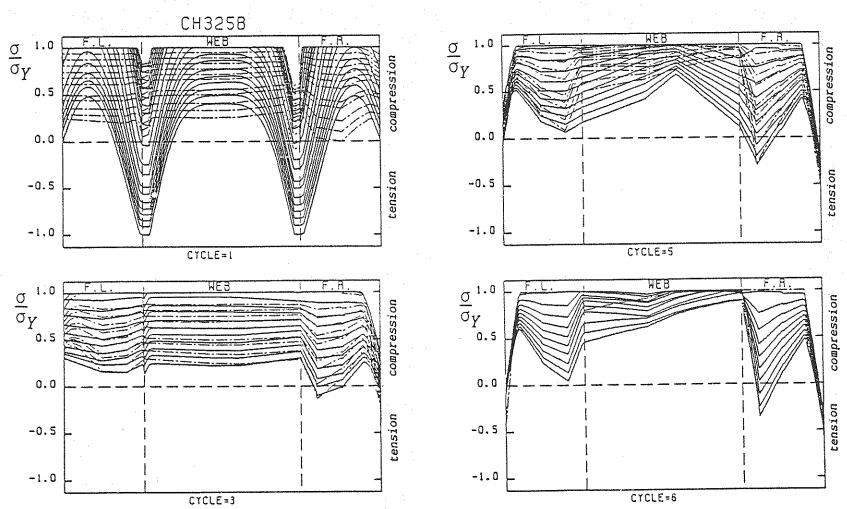

Fig. 6 Axial Stress Distributions calculated for Different Load Levels from Readings of Axial Strains of CH 325 B.

Table 4 Deterioration due to Repetitive Compression.

R	0.65	0.90	0.91	1.26	1.28	1.78
Specimen Type	CH455	CH325	CH457	CH235	CH327	CH237
Specimen Name	A,B,C	A,B	A,B,C	B	A,B	A,B
Maximum Load*	1.068	1.011	0.986	0.920	0.823	0.830
Δ (%) **	5.9	3.6	1.3	1.5	0.9	0.8

* The maximum load is non-dimensionalized by the yielding load.

** Δ refers to the average rate of the reduction of the peak load in each cycle to the maximum load, and may be conveniently called the deteriorating rate.

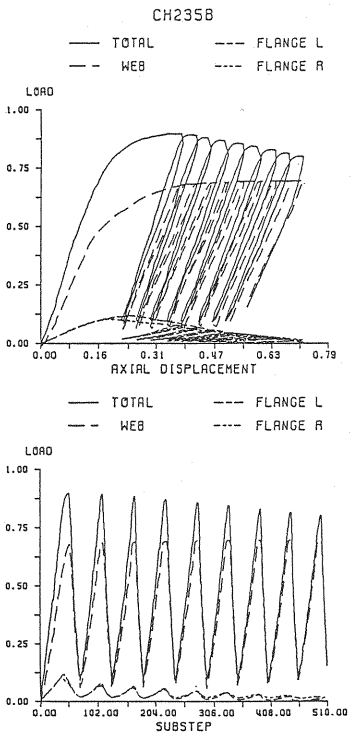

Fig. 7 Load-Displacement & Load-Substep Curves. CH 235 B.

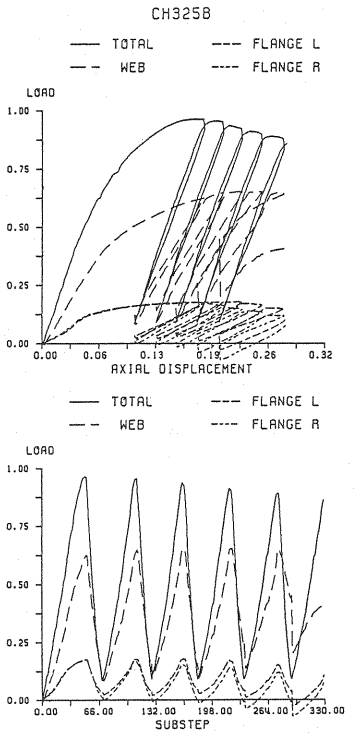

Fig. 8 Load-Displacement & Load-Substep Curves. CH 325 B.

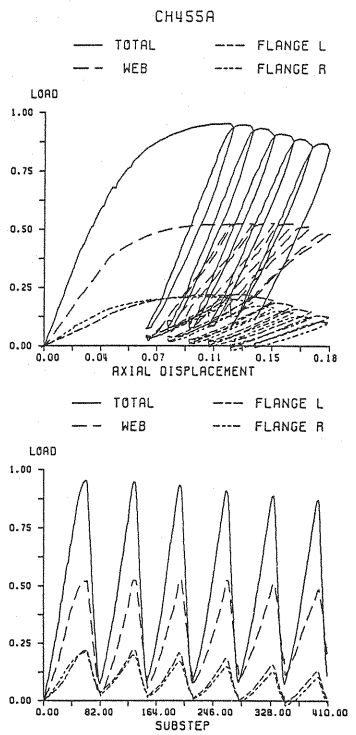

Fig. 9 Load-Displacement & Load-Substep Curves. CH 455 A.

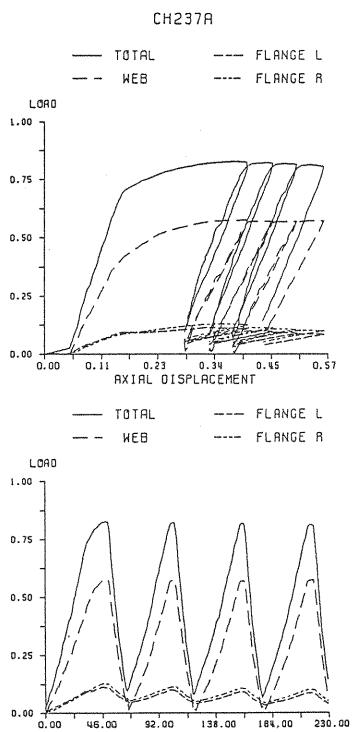

Fig. 10 Load-Displacement & Load-Substep Curves. CH 237 A.

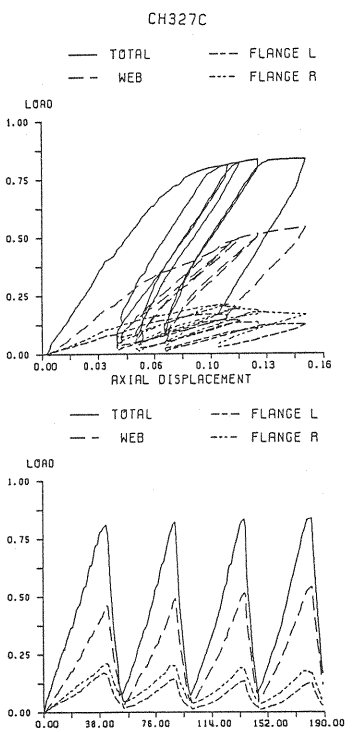

Fig. 11 Load-Displacement & Load-Substep Curves. CH 327 C.

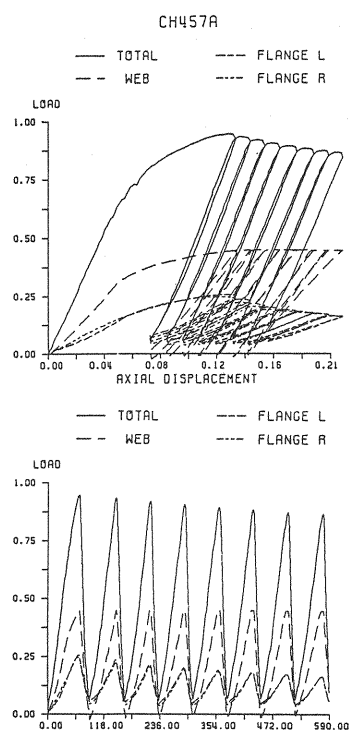

Fig. 12 Load-Displacement & Load-Substep Curves. CH 457 A.

the non-dimensionalized axial displacement by the thickness of the flange for each type of the test specimens, where distinctions are made with respect to either the total load, the load carried by the web and that by the flanges by the solid lines, broken lines and the dotted lines, respectively. Shown together are the loading history being the relationship between the load and the substeps. The reduction of the overall strength of the specimen is seen to be mainly caused by that of the flange plate due to its local buckling.

Table 4 shows the deterioration characteristics due to the repetitive compression for each value of the generalized slenderness ratio, R, of the flange plate. In this table, Δ refers to the average rate of the reduction of the peak load in each cycle to the maximum load, and may be conveniently called the "deteriorating rate". It is found that the larger the slenderness of the specimen, the smaller the deteriorating rate becomes, although the maximum load, namely, the magnitude of the first peak load decreases as the slenderness increases.

(3) Comparison with theoretical predictions

In this study the buckling loads were evaluated by Bleich's formula, Eq. (1). In his formula, the effect of the residual stresses is taken into account in the form similar to the Johnson's Parabola on the basis of the proportional limit :[7]

$$\sqrt{\tau}=\frac{\sigma_E(\sigma_Y-\sigma_E)}{\sigma_P(\sigma_Y-\sigma_P)} \quad \cdots\cdots (2)$$

where σ_E, σ_P and σ_Y refer to the Euler stress, the proportional limit and the yielding stress, respectively. Based on the buckling load thus obtained, the reduction of the strength due to the existence of the initial imperfections can be evaluated in the form of the imperfection sensitivity curves through the new unified approach[8)~10)].

Table 5 gives the comparison of the experimental ultimate loads with the Bleich's buckling loads[7]. Also, Fig. 13 shows the same results of the local flange plates for overall channel specimens. It is found that the Bleich's predictions are in good correlation with the corresponding test loads.

Figs. 14 to 19 show the relationship between the strength non-dimensionalized by the yielding strength and the initial out-of-plane deflection non-dimensionalized by the thickness of the flange plate for each cycle of each test column, together with the imperfection sensitivity curves predicted by the unified approach[8)~10)]. It is to be noted that the residual out-of-plane deflections of flange plates become

Table 5 Bleich's Loads and Experimental Ultimate Loads.

Ultimate Strength	Theoretical Load P_{th}			Experimental Load P_{ex}			P_{ex}/P_{th}		
Specimen	Total (tf)	Flange R (tf)	Flange L (tf)	Total (tf)	Flange R (tf)	Flange L (tf)	Total	Flange	Flange
CH235A	21.60	2.97	2.92	22.96	2.52	2.78	1.06	0.85	0.95
CH235B	21.00	2.90	2.85	20.43	2.30	2.60	0.97	0.79	0.91
CH235C	21.04	2.88	2.90	19.98	2.65	2.70	0.95	0.92	0.93
CH325A	23.81	4.18	4.18	25.34	4.27	3.61	1.06	1.02	0.86
CH325B	23.58	4.18	4.18	23.36	4.22	4.30	0.99	1.01	1.03
CH325C	23.79	4.14	4.14	22.24	4.20	4.15	0.93	1.01	1.00
CH455A	29.12	6.35	6.35	28.11	6.02	6.44	0.97	0.95	1.01
CH455B	28.70	6.35	6.27	29.41	6.35	6.46	1.02	1.00	1.03
CH455C	29.06	6.34	6.29	32.04	6.38	6.38	1.10	1.01	1.01
CH237A	18.92	3.34	3.34	20.83	3.50	3.30	1.10	1.05	0.99
CH237B	18.33	3.13	3.13	20.53	3.84	3.22	1.12	1.23	1.03
CH237C	18.85	3.19	3.19	20.45	3.22	3.19	1.08	1.01	1.00
CH327A	24.96	5.45	5.43	22.34	5.71	5.08	0.86	1.05	0.94
CH327B	24.83	5.44	5.47	23.30	4.93	5.58	0.94	0.91	1.02
CH327C	25.27	5.47	5.47	22.45	5.79	4.99	0.89	1.06	0.91
CH457A	32.71	8.55	8.55	32.44	8.47	8.74	0.99	0.99	1.02
CH457B	32.66	8.63	8.60	31.20	8.33	7.08	0.96	0.97	0.82
CH457C	33.21	8.50	8.55	32.94	8.49	8.83	0.99	1.00	1.03

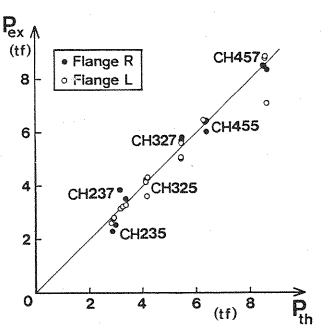

Fig. 13 Comparison of Bleich's Loads and Experimental Ultimate Loads for Local Flange Plates.

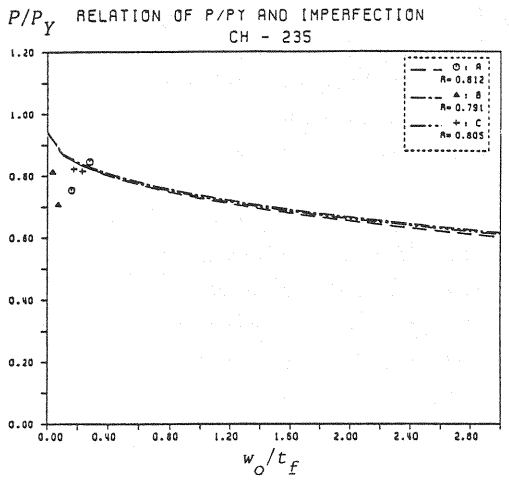

Fig. 14 Imperfection Sensitivity. CH235.

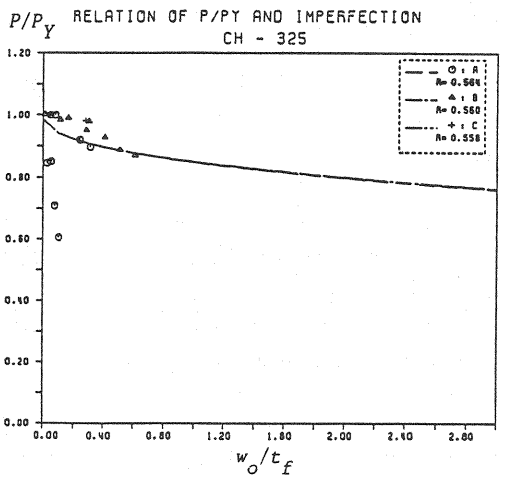

Fig. 15 Imperfection Sensitivity. CH325.

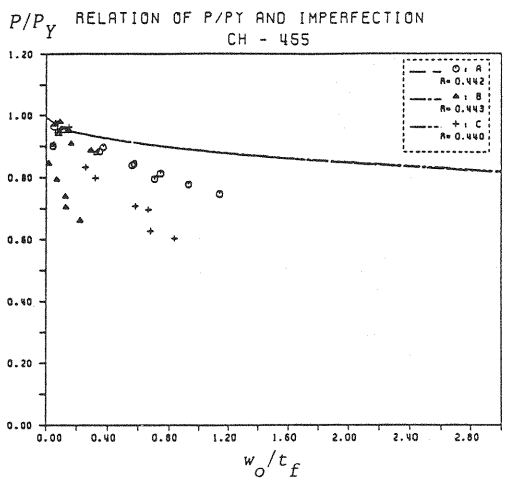

Fig. 16 Imperfection Sensitivity. CH455.

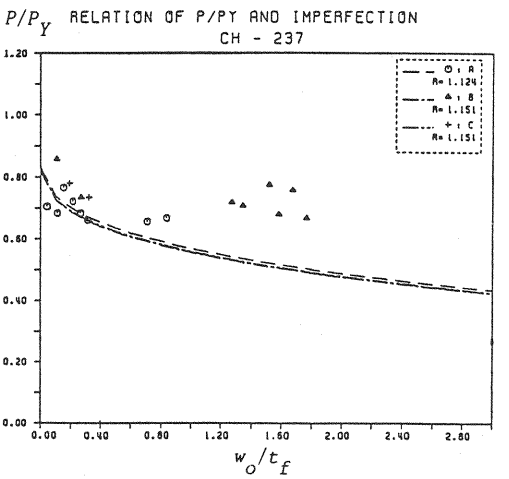

Fig. 17 Imperfection Sensitivity. CH237.

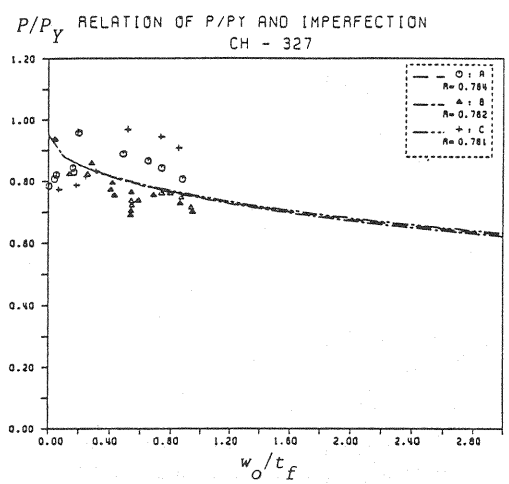

Fig. 18 Imperfection Sensitivity. CH327.

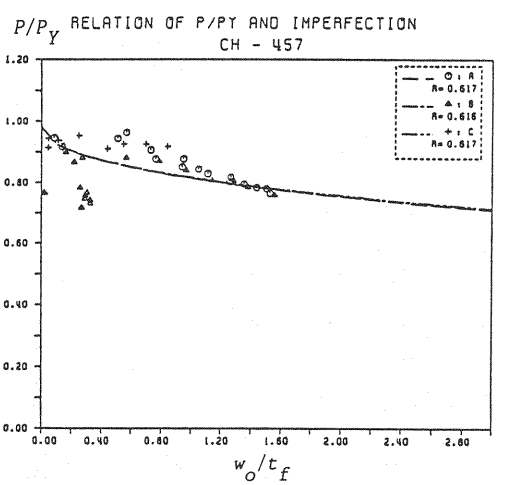

Fig. 19 Imperfection Sensitivity. CH457.

pronounced as the number of cycles increases. Also, it may be seen that the experimental values can be reasonably predicted by the theoretical imperfection sensitivity curves, although rigorously speaking, the theory does not take into account the fact that the residual stress distribution changes and is leveled off.

4. CONCLUSIONS

The following conclusions may be drawn from the study :

(1) The peak ultimate loads were precisely detected by the automated structural testing system. All of the specimens were unloaded in conformity with the criterion of the slope of the load-axial displacement curve. At the ultimate loads, the magnitude of the slope was very small or slightly less than zero indicating that the testing system worked accurately. Furthermore, these peak loads were found to be very close to those predicted by the Bleich's theory.

(2) As soon as the local plastic deformations were initiated, the torsional deformations became visible. This deformations became more pronounced as the load increased.

(3) The reduction of the total stub column strength due to repeated loading is mainly caused by that of the flange plates.

(4) The sheet piles with flange plates of smaller height have higher local buckling load, in general. However, the reduction of their strength becomes more pronounced, and its value depends largely on the aspect ratio of the flange plate.

(5) Due to repeated loading, the residual deformations tend to grow. This increment may be considered to be accelerated by the formation of the plastic failure mechanism which takes place at the first failure. On the other hand, the residual stresses tend to be leveled off as the number of cycles increases.

(6) The reduction of the strength during the loading history is found to be proportional to the square root of the corresponding initial out-of-plane deflections of flange plates. Thus, the concept of the "FOLD"-type imperfection sensitivity through the nonlinear bifurcation theory seems to be acceptable.

(7) The imperfection sensitivity stays small in the small range of the generalized width-thickness ratio, R, of the flange of the sheet pile ; however, it becomes vulnerable to the torsional deformation because of high axial stress. The effect of the residual stress is not generally significant near $R=0.7$; however, the strength is reduced remarkably by a slight increment of the imperfection. From the design point of view, the buckling strength should be high enough; besides, the imperfection sensitivity should be kept as small as possible. In this respect, the value of parameter R may be conveniently taken to be not too far from unity as in the case of the current design of wider web cross section of sheet piles.

ACKNOWLEDGMENTS

The authors wish to express appreciation to President Yoshiji Niwa of Fukui National College of Technology and the Emeritus Professor of Kyoto University for his support and valuable suggestions.

This study accepted a Grant-in-aid for Developmental Scientific Research from the Ministry of Education, Science and Culture in 1981 through 1982 and was financially assisted by Kawasaki Steelwork, Inc. in 1982.

REFERENCES

1) Ohkata, S. : On the compressive strength of U-shaped steel sheet piles, Technical Report of Kawasaki Steelwork, Vol. 8, No. 1, pp. 109~115, 1976 (in Japanese).
2) Popov, Egor P. and Petersson, H. : Cyclic metal plasticity : Experiments and theory, Proc. of ASCE, Vol. 104, No. EM 6, pp. 1371~1388, 1978.
3) Seeger, T., Hoffmann, M. und Klee, S. : Die Beurteilung der Bauteilschwingfestigkeit auf der Basis örtlicher Beanspruchungungen, Kurt-Klöppel-Gedachtnis-Kolloquium, THD-Schriftenreihe Wissenschaft und Technik, S. 409~448, 1986.
4) Uetani, K. : Symmetry limit theory and steady-state limit theory for beam-columns subjected to alternating plastic bending, Doctoral Dissertation, Kyoto University, 1984.

5) Niwa, Y., Watanabe, E. and Isami, H. : Automated structural testing using microcomputer system, Proc. of JSCE, No. 332, pp. 145～158, 1983.
6) Niwa, Y., Watanabe, E. and Isami, H. : Automated testing of thin-walled steel structures under repetitive loading by microcomputer system, Proceedings of the 2nd International Conference on Civil and Structural Engineering Computing, Vol. 2, pp. 337～343, 1985.
7) Bleich, F. : Buckling strength of metal structures, McGraw-Hill, 1952.
8) Niwa, Y., Watanabe, E., Isami, H. and Fukumori, Y. : A new approach to predict the strength of compressed steel plates, Proc. of JSCE, No. 341, pp. 23～30, 1984.
9) Niwa, Y., Watanabe, E. and Isami, H. : A unified view on the strength of columns, beams and compressed plates through catastrophe theory, Proc. 3rd International Colloquium on Stability of Metal Structures, Paris, Preliminary Report, 1983.
10) Niwa, Y., Watanabe, E. and Isami, H. : A unified approach to predict the strength of steel structures, Theoretical and Applied Mechanics, Vol. 34, pp. 265～273, 1986.

(Received December 3 1986)